IEEE Journal of Translational Engineering in Health and Medicine

Received 8 May 2014; revised 6 September 2014 and 15 October 2014; accepted 18 December 2014. Date of publication 16 January 2015; date of current version 27 January 2015.

Digital Object Identifier 10.1109/JTEHM.2015.2389230

Development of Point of Care Testing Device for Neurovascular Coupling From Simultaneous Recording of EEG and NIRS During Anodal Transcranial Direct Current Stimulation

UTKARSH JINDAL[1], MEHAK SOOD[1], ANIRBAN DUTTA[2], (Member, IEEE), AND SHUBHAJIT ROY CHOWDHURY[1], (Member, IEEE)

[1]Centre for VLSI and Embedded Systems Technology, International Institute of Information Technology Hyderabad, Hyderabad 500032, India
[2]Institut national de recherche en informatique et en automatique, Montpellier 34095, France

CORRESPONDING AUTHOR: S. R. CHOWDHURY (src.vlsi@iiit.ac.in)

This work was supported in part by the Department of Science and Technology through the Government of India and in part by the Franco-Indian INRIA-DST Associate Team support 2014–2017.

ABSTRACT This paper presents a point of care testing device for neurovascular coupling (NVC) from simultaneous recording of electroencephalogram (EEG) and near infrared spectroscopy (NIRS) during anodal transcranial direct current stimulation (tDCS). Here, anodal tDCS modulated cortical neural activity leading to hemodynamic response can be used to identify the impaired cerebral microvessels functionality. The impairments in the cerebral microvessels functionality may lead to impairments in the cerebrovascular reactivity (CVR), where severely reduced CVR predicts the chances of transient ischemic attack and ipsilateral stroke. The neural and hemodynamic responses to anodal tDCS were studied through joint imaging with EEG and NIRS, where NIRS provided optical measurement of changes in tissue oxy-(*HbO*2) and deoxy-(*Hb*) hemoglobin concentration and EEG captured alterations in the underlying neuronal current generators. Then, a cross-correlation method for the assessment of NVC underlying the site of anodal tDCS is presented. The feasibility studies on healthy subjects and stroke survivors showed detectable changes in the EEG and the NIRS responses to a 0.526 A/m^2 of anodal tDCS. The NIRS system was bench tested on 15 healthy subjects that showed a statistically significant ($p < 0.01$) difference in the signal-to-noise ratio (SNR) between the ON- and OFF-states of anodal tDCS where the mean SNR of the NIRS device was found to be 42.33 ± 1.33 dB in the ON-state and 40.67 ± 1.23 dB in the OFF-state. Moreover, the clinical study conducted on 14 stroke survivors revealed that the lesioned hemisphere with impaired circulation showed significantly ($p < 0.01$) less change in *HbO*2 than the nonlesioned side in response to anodal tDCS. The EEG study on healthy subjects showed a statistically significant ($p < 0.05$) decrease around individual alpha frequency in the alpha band (8–13 Hz) following anodal tDCS. Moreover, the joint EEG-NIRS imaging on 4 stroke survivors showed an immediate increase in the theta band (4–8 Hz) EEG activity after the start of anodal tDCS at the nonlesioned hemisphere. Furthermore, cross-correlation function revealed a significant (95% confidence interval) negative cross correlation only at the nonlesioned hemisphere during anodal tDCS, where the log-transformed mean-power of EEG within 0.5–11.25 Hz lagged *HbO*2 response in one of the stroke survivors with white matter lesions. Therefore, it was concluded that the anodal tDCS can perturb the local neural and the vascular activity (via NVC) which can be used for assessing regional NVC functionality where confirmatory clinical studies are required.

INDEX TERMS Electroencephalogram, near infrared spectroscopy, transcranial direct current stimulation, Hilbert-Huang transform, neurovascular coupling, stroke, small vessel diseases.

I. INTRODUCTION

Stroke or cerebrovascular accident is caused when an artery carrying blood from heart to an area in the brain bursts or a clot obstructs the blood flow thereby preventing delivery of oxygen and nutrients. Worldwide, 15 million people suffer a stroke every year, where Indian studies have estimated that the incidence rates increase from 27-34/100,000 in the 35-44 age group to 822-1116/100,000 in the 75+ age group [1]–[3]. Moreover, ischemic stroke is the leading cause of morbidity and long term disability across the world, and is among the leading causes of death [4]. It is also the second leading cause of dementia (after Alzheimer's disease). The projected cost of patient care for stroke will reach trillions of dollars over the next five decades. Stroke accounts for nearly 10% of deaths and about 5% of health-care costs [5]. The total direct and indirect cost of cardiovascular disease (CVD) and stroke in the United States for 2010 is estimated to be $315.4 billion [6]. This figure includes health expenditures (direct costs, which include the cost of physicians and other professionals, hospital services, prescribed medications, home health care, and other medical durables) and lost productivity that results from premature mortality (indirect costs). In India, stroke in younger individuals is high (18-32% of all stroke cases) compared with high-income countries that presents a greater burden on the quality of life [1], [7]. Stroke drastically affects the economical productivity of that younger age group, adding further to the disease burden [7]. With increasing number of younger person with stroke and an aging population, the human as well as the economic burden of stroke and small vessel disease on health systems is likely to dramatically increase in future which is a hidden epidemic for India [8]. In fact, elderly population in India is predicted to increase to 12% of the total population by 2025 [9] where age is the primary risk factor. Consequently, Indian health ministry's working group noted that ''India will soon become home to the second largest number of elderly in the world. The challenges are unique with this population in India.'' Therefore, low-cost innovative methodologies for prognosis and monitoring of stroke and small vessel disease are urgently required in India that avoids transportation of critically ill patients and provides home-based intervention.

Cross-sectional studies suggest that impaired cerebral haemodynamics precedes ischemic stroke and transient ischaemic attack (TIA) where cerebrovascular reactivity (CVR) reflects the capacity of blood vessels to dilate, and is an important marker for brain vascular reserve [10]. CVR provides an useful addition to the traditional baseline blood flow measurement where severely reduced CVR predicts the risk of ipsilateral stroke and TIA [10]. Also, neural activity is closely related, spatially and temporally, to cerebral blood flow (CBF) that supplies glucose via neurovascular coupling. However, neurological symptoms may not be visible until CBF drops to 40% of normal, and prolonged periods of cerebral ischemia increase the likelihood that neurological symptoms will become irreversible as CBF further drops to 20% of normal [11], [12]. The goal of most medical interventions in acute ischemic stroke care is to maximize blood perfusion in the lesioned region and surrounding ischemic penumbra by increasing local and/or global CBF. Intervention strategies to increase CBF are based on the premise that normal auto-regulation of CBF is disrupted and perfusions of the infarcted and penumbral regions are dependent on perfusion pressure [13], [14]. Here, the ability to directly or indirectly measure CBF, concentrations of oxy- and deoxy-hemoglobin at the point-of-care/bedside would provide new opportunities for monitoring cerebro-vascular autoregulation in early stroke/TIA, permitting hemodynamic interventions to be optimized, and potentially administered before the onset of neurological symptoms. Furthermore, because of the high prevalence of stroke and small vessel disease, and the enormous cost of its management, even strategies with modest benefits are worth pursuing to ameliorate impairments in CBF that may lead to neural impairments leading to Mild Cognitive Impairment (MCI) [15]. Moreover, impaired cerebral haemodynamics may lead to vascular dementia (VD), where the pathophysiological links between VD and Alzheimer disease (AD) has been widely discussed [15], [16]. In fact, an association was found between impaired cerebral microvessels functionality (elucidated with CVR) and unfavorable evolution of cognitive function in patients with AD [16].

Functional near infrared spectroscopy (fNIRS) is based on the optical measurement of changes in tissue oxy-($HbO2$), and deoxy-(Hb) haemoglobin concentration [17] whereas cerebral oximetry is cerebral oxygenation monitoring via near-infrared spectroscopy (NIRS) [18]. One aspect of this response—the blood oxygen level dependent (BOLD) signal is the basis for functional magnetic resonance imaging (fMRI), a brain imaging modality closely related to fNIRS in terms of the underlying measurand. The responses measuring during fNIRS are usually interpreted in terms of changes in $HbO2$ and Hb concentration — a somewhat richer set of variables than those available from basic fMRI. A third hemodynamic variable, Hbt, can be derived as the sum of $HbO2$ and Hb concentrations, which is considered a good indicator of the variations in the regional cerebral blood volume (CBV) [19]. In this study, we used anodal transcranial direct current stimulation (tDCS) to evoke haemodynamic response based on prior work [20] that showed a significant correlation between current strength and the increase in regional cerebral blood flow (CBF) in the on-period relative to the pre-stimulation baseline. Therefore, the first objective was to develop a 4-channel NIRS-based hardware to estimate changes in cerebral oxygenation evoked by anodal tDCS and to evaluate the feasibility of tDCS-evoked hemodynamic response in 15 healthy subjects. After feasibility testing, it was postulated that the lesioned hemisphere would have reduced tDCS-evoked hemodynamic response than the non-lesioned hemisphere. This hypothesis was evaluated towards discrimination between the lesioned and non-lesioned hemisphere in 14 stroke survivors.

As in fMRI, an interpretation of the hemodynamic responses is often considered on the simple basis that

IEEE Journal of Translational Engineering in Health and Medicine

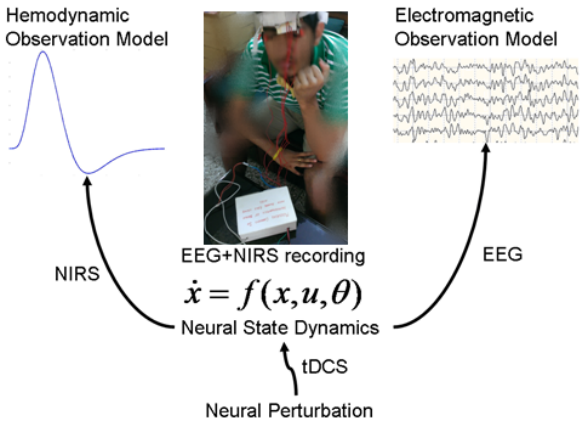

FIGURE 1. EEG-NIRS based simultaneous recording [24] of the hemodynamic and electromagnetic responses to perturbations with tDCS [25].

significant changes in hemodynamics corresponds to increases in cortical neural activity [21] where tDCS can up- and down-regulate cortical excitability depending on current direction [20]. During cortical neural activity, the electric currents from all excitable membranes of brain tissue superimpose at a given location in the extracellular medium and generate a potential, which is referred to as the electroencephalogram (EEG) when recorded from the scalp [22]. Quantitative EEG analysis has been used as a method of identifying subclinical brain injury during neurosurgical procedures, such as carotid endarterectomy, and for ischemia detection, global function assessment, medication titration, and prognostication [23]. Furthermore, high multilevel reproducibility has been shown [24] where EEG parameters reliably discriminated between stroke and transient ischaemic attack (TIA) patients or control subjects, and correlated significantly with clinical and radiological status. Reliable EEG parameters can be evaluated in a general stroke population for clinically relevant state and outcome measures [24]. There are several studies that investigated the relationship between EEG alpha rhythm variations (alpha rhythm lies in the range of 8 to 13 Hz) and baseline regional CBF differences [25]. where the hemodynamic responses associated with cortical neural activity, i.e., the relationship between local neural activity and cerebral blood flow is termed neurovascular coupling (NVC) [26]. Therefore, EEG may provide a measure that is independent from fNIRS where EEG can be used to indirectly detect and monitor CBF. Here, simultaneous EEG-NIRS imaging [27] during perturbation with tDCS may help us in understanding the NVC underlying neural and hemodynamic responses post-stroke. Furthermore, EEG-NIRS joint imaging may improve the specificity by estimating NVC as a biomarker for post-stroke impaired cerebral microvessels functionality (see Figure 1) [28] where non-neuronal systemic physiological fluctuations often contaminate fNIRS signals. Therefore, the second objective was development of a 5-channel EEG hardware which was bench tested by 10 healthy subjects. Then, the 5-channel EEG hardware was integrated with NIRS for EEG-NIRS based modeling of NVC underlying the response to anodal tDCS. The feasibility testing was conducted on 4 stroke survivors.

EEG-NIRS based modeling of NVC was based on prior work that showed tDCS induced changes in neuronal membrane potentials in a polarity-dependent manner and induced synaptically driven after-effects after a sufficient duration [25]. The activated synapse results in local excitatory postsynaptic current (EPSC), which then results in an excitatory postsynaptic potential (EPSP) at the cell body causing alterations in membrane potential. The synaptic transmembrane current is a major contributor of the extracellular signal that can be measured with current source density (CSD) analysis of the extracellular field potentials viz. local field potentials (LFP) [26]. In our case, EEG measured the extracellular field potentials which were used to estimate the EEG surface laplacian [27] - the magnitude of the radial (transcranial) current flow leaving (sinks) and entering (sources) the scalp. These reference-free current source density (CSD) waveforms yield measures that more closely represent underlying neuronal current generators [28]. Therefore, CSD waveform at the site of stimulation should represent the underlying neuronal current generators during anodal tDCS. Here, our prior work showed an increase of fractional power in the Theta band (4-8Hz) immediately after stimulation and decrease around "individual alpha frequency" in the Alpha band (8-13Hz) following anodal tDCS [20]. We proposed an EEG-NIRS based imaging of tDCS evoked neural and hemodynamic responses [33] where tDCS has been shown to induce polarity-specific changes of cortical blood perfusion [34] and neural activity [29]. Parts of this work have been presented earlier in conferences [28], [35], [36].

In this translational study, we present low-cost 1) development of a 4-channel NIRS-based hardware to estimate cerebral oxygenation, 2) development of a 5-channel EEG hardware to estimate the surface Laplacian [30] - the magnitude of the radial (transcranial) current flow leaving (sinks) or entering (sources) the scalp, 3) an EEG-NIRS based modeling approach to estimate NVC underlying the response to anodal tDCS. Here, stimulation by tDCS allows to perturb the neurovascular state of focal cortical tissue and localize the lesioned brain areas which is a novel approach. This has significant clinical scope since cross-sectional studies suggest that impaired cerebral haemodynamics precedes stroke and TIA where cerebrovascular reactivity (CVR) reflects the capacity of blood vessels to dilate, and is an important marker for brain vascular reserve [24]. Moreover, impairments in CBF may lead to neural impairments leading to Mild Cognitive Impairment (MCI) [6]. Here, tDCS-evoked CVR (captured with fNIRS) and EEG reactivity may provide an useful addition to the traditional baseline blood flow measurement where severely reduced reactivity may predict the risk of ipsilateral stroke and TIA [24].

II. METHODS AND PROCEDURES

In our earlier work, it has been shown that anodal tDCS enhanced activity and excitability of the excitatory pyramidal

neuron at a population level in a non-specific manner, where μ -rhythm desynchronization was found to be generated [20]. Also, our case study [21] showed detectable hemodynamic response (0-60sec) to a 0.526A/m^2 square-pulse (0-30sec) of anodal tDCS where it was postulated that alterations in the vascular system may result in secondary changes in the cortical excitability. Based on these preliminary studies, we proposed EEG-NIRS based low-cost screening and monitoring of cerebral microvessels functionality under perturbation with tDCS [22]. The objective of this method study was to develop a low-cost point-of-care-testing device [23] and to present a method to assess NVC based on simultaneous EEG-NIRS recordings.

A. DEVELOPMENT OF PHANTOMS FOR BENCH-TESTING NIRS DEVICE

The NIRS instrumentation needs to be calibrated using phantoms [37]–[40]. Typically, phantoms are static in nature and contain a fixed value for the NIRS instrument to measure in order to validate that the device is working properly [40]. However, the drawback with static phantoms is that these phantoms do not fully replicate human body. Oxygen levels in the body, brain or muscle for instance, are constantly changing depending on the task being performed [40]. Therefore, phantoms that have the ability to change the properties being measured provide greater realistic simulation. These dynamic phantoms give researchers a better understanding of what the NIRS data should look like when data acquisition takes place [40]. In the current work, a dynamic phantom was developed for our NIRS system.

The initial step in designing a dynamic phantom was to calculate the correct amount of scattering and absorption agents in order to obtain the optical coefficients of absorption (μ_a) and scattering (μ_s) resembling human brain, which according to literature were 0.16 cm^{-1} and 6.9 cm^{-1} respectively [40]. In our study, titanium dioxide was used as the scattering agent. Photon migration imaging (PMI) toolbox was used to validate the proper dimensions needed for the phantom [41]. In order to incorporate the dynamic properties to the phantom, liquid crystal (LC) paint was added to the surface of a 500ml blank phantom of pure paraffin wax. The LC paint has the ability to change its color depending on the temperature of the paint. While the paint is translucent at room temperature (20 °C - 25 °C), the paint becomes darker outside this temperature range. To heat the paint, a resistive wire mesh was placed on top of the paint and electric current was applied to the wire to generate Joule heating thereby changing the optical properties (μa, μs) of the phantom.

B. DEVELOPMENT OF THE NIRS DEVICE

The basic design of the NIRS device is shown in Figure 2. Three NIR sources and three detectors have been used. NIRS is an optical measurement and therefore it is the changes in the optical properties of the tissue volume during neural activation that induces signal changes. Consequently, a spectrophotometric modeling component is required to capture this

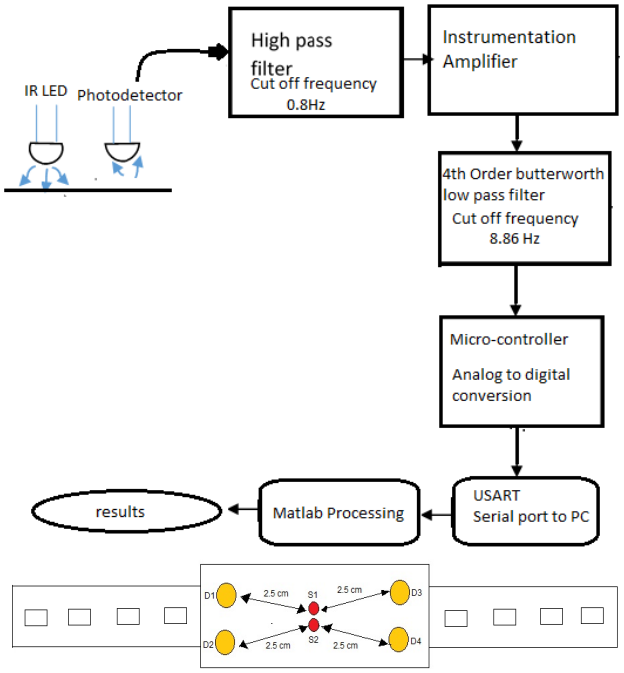

FIGURE 2. Top Panel: Block diagram of the NIRS system. Bottom Panel: Design of NIRS probe.

aspect of the signal. The signal acquired at the detector can be approximated as a linear mixture of a number of components. Differential spectroscopy has been used to obtain relative changes in the concentrations of the two chromophores, viz. oxy-hemoglobin and deoxy-hemoglobin, making it possible to identify whether changes in oxygen saturation result from changes in blood volume or changes in oxygen consumption. An increase/decrease in blood volume causes an increase/decrease in total hemoglobin concentration which in turn causes a change in oxygen saturation. Changes in oxygen consumption are reflected by changes in oxy- and deoxy-hemoglobin concentrations in opposite directions such that the total hemoglobin concentration stays the same. The wavelengths used in our experiment were 770nm and 850nm. The alignment of the light emitting diode (LED) and photodetectors are shown in Figure 1. In Figure 1, S1 and S2 indicate LED and D1, D2, D3 and D4 are photo-detectors. The distance between the source and detector was maintained at 2.5cm.

The tDCS is a form of electrical stimulation which uses constant low amplitude electrical current that is delivered transcranially via sponge (conductive rubber-core electrode) soaked with normal (0.9%) saline solution. We delivered a current density of 0.526A/m^2 for 3 minutes for tDCS. The anode (positive polarity electrode) was placed at Cz (International 10-20 system of scalp sites) and the cathode (negative polarity electrode) was placed at either F3 or F4 (International 10-20 system of scalp sites) for left or right side stimulation respectively. The signal has been acquired on both the left and right side of the cerebral frontal cortex before and after anodal tDCS, using 770nm/850nm dual

LED in the experiment. Modified Beer Lambert's Law was used to relate the chromophore concentration to the optical absorption values. The feasibility of hemodynamic response to anodal tDCS was evaluated by 15 healthy subjects (age group of 20-30 years), i.e., the NIRS-tDCS healthy study at the International Institute of Information Technology - Hyderabad, India. The hypothesis that the lesioned hemisphere would have reduced tDCS-evoked hemodynamic response was evaluated in 14 stroke survivors (age group 42-73 years), i.e., the NIRS-tDCS stroke study at the Institute of Neurosciences, Kolkata.

Subjects were recruited after ethics approval and experiments were conducted after taking informed consent, conforming to the Declaration of Helsinki. Participants were seated in a quiet room and their eyes were open and fixated on a point on the wall in front of them during the entire experiment. The total testing time was roughly 14 minutes. NIRS was performed for two minutes on the F3 site followed by anodal tDCS for three minutes. After anodal tDCS, NIRS was performed again to measure the hemodynamic changes as a result of anodal tDCS. Therefore, the NIRS data was collected for 2 minutes pre- and post- tDCS. The same process was repeated with the F4 site. Analog arterial pressure data from the operating room hemodynamic monitor and the NIRS signals were both sampled at 60 Hz. These signals were time integrated as non overlapping 10sec mean values, which is equivalent to a non-overlapping moving average filter with a 10sec time window re-sampled at 0.1 Hz. The objective was to eliminate high frequency noise from the respiratory and pulse frequencies thus allowing detection of oscillations and transients below 0.05 Hz. The signals were further high pass filtered with a cut off at 0.003Hz to remove slow drifts. The change in the signal to noise ratio (SNR), i.e. the ratio between signal power and noise power in the overall NIR signal, between the on and off phases of the anodal tDCS was investigated. The background noise is the recording when the device was not interfaced with the skin. A paired t-test (MATLAB function ''ttest'') was performed to find any significant difference in the SNR values between the on and off phases of the anodal tDCS in order to confirm haemodynamics response to tDCS in 15 healthy subjects (age group of 20-30 years). Then, 14 patients with established and acute ischemic stroke (<1 month) localized to a single hemisphere (10 male and 4 females from age 42 to 73) were recruited to study any difference in the hemodynamic response of the lesioned and non-lesioned hemisphere during perturbation with anodal tDCS. A paired t-test (MATLAB function ''ttest'') was performed to find any significant differences.

C. DEVELOPMENT OF THE EEG DEVICE

The EEG Front-End (EEG-FE) from Texas Instruments (Texas Instruments, Inc.) that is based on ADS1299 - an eight-channel, 24-bit, low-power; integrated analog front-end designed for EEG applications - was used in this study. The motherboard allowed the EEG-FE to be connected to a battery-operated laptop computer via an available USB port. Due to the extremely low input-referred noise of the ADS1299, it allows for direct interface to EEG biopotential signals. With a typical noise of 1μVP-P and a 70Hz input bandwidth, this was a 77% reduction in currently existing medical analog Front-Ends. The graphical user interface (see Figure 3) was developed in LabVIEW (short for Laboratory Virtual Instrument Engineering Workbench) which is a system-design platform and development environment for a visual programming language from National Instruments (National Instruments, USA).

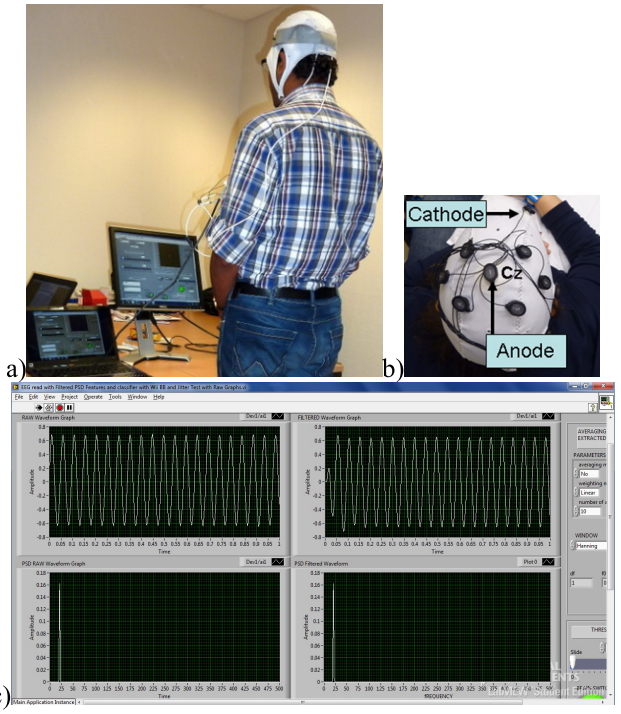

FIGURE 3. Bench-testing of the EEG device. a) test setup, b) EEG montage with tDCS Anode and Cathode, c) LabVIEW user interface.

Five healthy males and five healthy females aged between 22 to 46 years volunteered for the feasibility study, i.e., the EEG-tDCS healthy study at the University of Medicine Goettingen, Germany and the Institut national de recherche en informatique et en automatique, France. Experiments were conducted after taking informed consent, conforming to the Declaration of Helsinki. Participants were seated in a quiet room with their eyes open and fixated on a point on the wall in front of them during the entire experiment. Anodal tDCS was conducted for 15min (current density=0.526A/m^2) with the anode positioned at Cz (international 10-20 system of scalp sites) and cathode over left supraorbital notch. Eyes-open resting state EEG was recorded at 500Hz from the central site Cz (international 10-20 system of scalp sites) and the nearby electrodes F3, F4, P3, P4 (international 10-20 system of scalp sites) before and immediately after anodal tDCS at Cz. At Cz, the surface Laplacian was computed [30] which provided the magnitude of the radial (transcranial) current flow leaving (sinks) or entering (sources) the scalp.

From EEG recordings before and after anodal tDCS, the average experimental power spectrum was analyzed from 0.25Hz to 50Hz for 25 successive 4s artifact-free epochs (i.e., 100sec immediately before and 100sec immediately after anodal tDCS) using Welch's averaged, modified periodogram spectral estimation method (MATLAB function "spectrum.welch").

D. ESTIMATION OF NEUROVASCULAR COUPLING FROM EEG-NIRS SIMULTANEOUS IMAGING DURING TDCS

Prior works show a strong coupling between local field potentials (LFP) and regional vascular responses even in the absence of spikes (i.e., subthreshold depolarization) [29]. This regional vascular response was estimated using NIRS that measured changes in (cortical) tissue oxy-(*HbO*2), and deoxy-(*Hb*) haemoglobin concentration roughly underlying the stimulation location. Here, our prior work found an initial dip in *HbO*2 at the beginning of anodal tDCS that corresponded with an increase in the log-transformed mean-power of EEG within 0.5Hz-11.25Hz frequency band [28], [43]. Moreover, our preliminary study showed an increase of fractional power in the Theta band (4-8Hz) and decrease around "individual alpha frequency" in the Alpha band (8-13Hz) at the stimulation site following anodal tDCS [36].

TABLE 1. Summary of the case series (M: male, F: female, MCA: middle cerebral artery, CABG: coronary artery bypass graft).

Case	Age/ gender	MRI diagnosis	Comorbidities	Year of stroke
1	31/M	Right MCA	White matter hyperintensities	2008
2	63/M	Left MCA	Diabetis, Hypertension	2009
3	73/M	Left MCA	Post-CABG	2010

Based on our preliminary results [28], [35], [36], [43], we developed a bi-hemispheric tDCS and simultaneous EEG-NIRS recording montage (see Figure 4). For the clinical study (see Table 1), we placed the EEG-NIRS/tDCS montage at the F3 and F4 sites for bi-hemispheric stimulation and recording, as shown in Figure 4. A current density of 0.526A/m^2 was delivered via 16cm^2 square sponge (conductive rubber-core electrode) soaked with normal (0.9%) saline solution. The anode and cathode for tDCS alternated between F3 and F4 sites to deliver 30sec of steady stimulation with 10sec of ramp-up and ramp-down (as shown in the bottom panel of Figure 4), which was repeated 15 times resulting in 1500sec of testing time. Simultaneous 8-channel EEG recordings were conducted via Ag/AgCl ring-electrode (impedance <5kOhms) using the EEG Front-End (EEG-FE) from Texas Instruments (Texas Instruments, Inc.) that is based on ADS1299. To reduce the cost of the NIRS montage, we used only four symmetrically-placed 770nm/850nm dual LED sources inserted through EEG ring-electrodes for each hemisphere in the lateral,

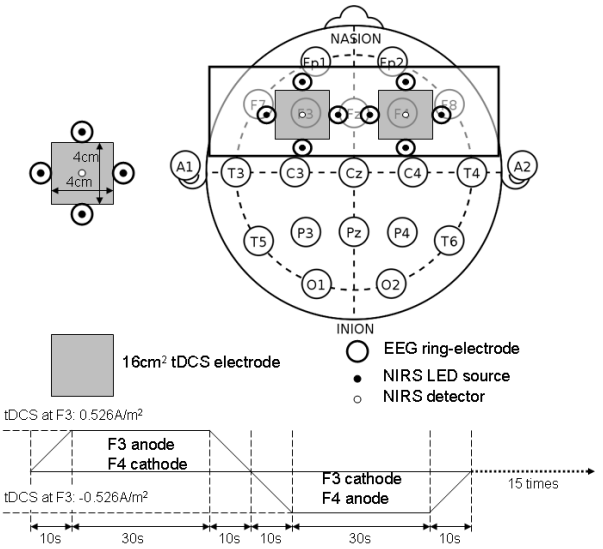

FIGURE 4. Bi-hemispheric tDCS and simultaneous EEG-NIRS recording montage.

medial, anterior and posterior directions from the detector at roughly 3.0cm source-detector separation.

Eyes-open block-averaged resting-state simultaneous NIRS and EEG recordings [27] were conducted during tDCS where we analyzed only the anodal tDCS data (30sec steady state stimulation). EEG from four symmetrically-placed ring-electrodes were interpolated with spherical splines to estimate the EEG at F3 and F4 sites (virtual electrode) using EEGLAB 'eeg_interp()' function [44]. For analysis of simultaneously acquired EEG and *HbO*2 waveforms at F3 and F4 sites, we developed a method for the assessment of neurovascular coupling at the site of anodal tDCS. We leveraged Empirical Mode Decomposition (EMD) of the EEG time series to break it into a set of intrinsic mode functions (IMFs) using Huang Hilbert Transform (HHT) [31]. The fact that IMFs are all in the time-domain and of the same length as the original EEG time series allows for varying frequency in time to be preserved. Generally, the first IMF contains the highest frequency components and the oscillatory frequencies decrease with increasing IMF index. The ith IMF for EEG is denoted as $IMF_{EEG,i}$ where only the ones that had instantaneous frequencies less than 11.25 Hz and greater than 0.5 Hz for the whole signal duration were selected based on our prior work [28], [43]. Cross-correlation function (CCF) was calculated during anodal tDCS between log-transformed mean-power time-course of $IMF_{EEG,i}$ and *HbO*2 time-series. CCF based assessment of the patient-specific status of NVC was conducted on four chronic (>6 months) ischemic stroke survivors (3 males, 1 female from age 31 to 76 (see Table 1), i.e., the NIRS/EEG-tDCS stroke study at the University of Medicine Goettingen, Germany and the Institut national de recherche en informatique et en automatique, France.

III. RESULTS

The phantom (size:20cm × 20cm × 10cm) that was developed in this study was analyzed for scattering coefficient

IEEE Journal of Translational Engineering in Health and Medicine

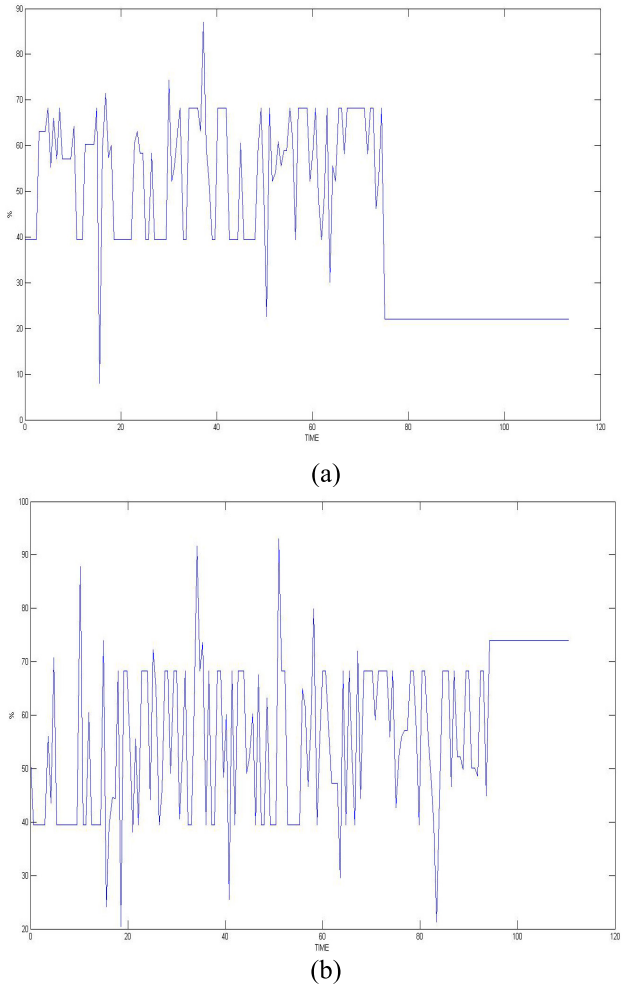

FIGURE 5. Phantom simulation results (time in seconds) for two different runs of the NIRS.

where a concentration of 0.367 moles/dm^3 of titanium dioxide in paraffin wax and yielded a scattering coefficient of 6.9 cm^{-1}. Figure 5 shows the phantom results on two different runs of the NIRS. The results of phantom simulation studies with our set up indicated 58% and 62% mean cerebral oxygen saturation when the optical properties of the phantom changed on being heated by the resistive mesh via current stimulation such that the temperature at the surface of phantom reaches in the range of 50-55 °C. The resistance value of resistive mesh is chosen to be of 275 ohms and the current was gradually increased to 3 amperes. The pulsating variations of the waveforms emulated the dynamic variation of cerebral oxygen saturation with arterial systole and diastole of the cerebro-vascular artery. The results were quite agreeable with the normal physiologic values of cerebral oxygen saturation in brain parenchyma [46]. In the 14 acute ischemic stroke (<1 month) survivors (NIRS-tDCS stroke study), the lesioned hemisphere with impaired circulation showed significantly less change in cerebral oxygen saturation than the non-lesioned side in response to anodal tDCS. There was a significant change in HbO2 in the non-lesioned side

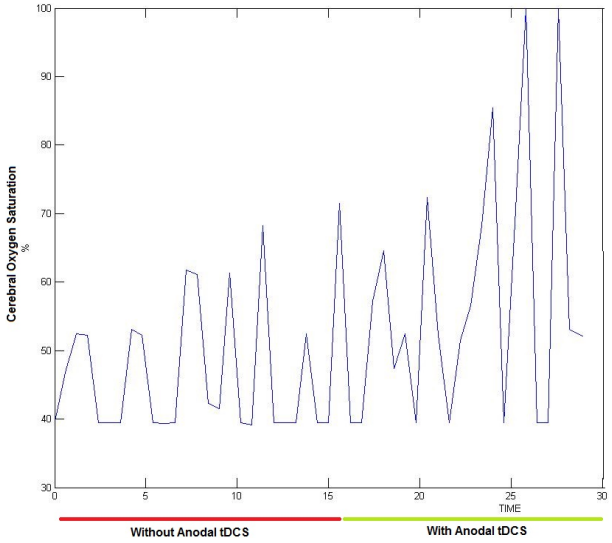

FIGURE 6. Change in the cerebral oxygen saturation with anodal tDCS in a subject (time in minutes).

[male: (3.43 ± 0.86) and female: (3.32 ± 0.74)] but not in the side with stroke lesion [male: (0.26 ± 0.28) and female: (0.24 ± 0.26)], $p < 0.01$ as is evident from figure 6. For the 4 stroke cases (NIRS/EEG-tDCS stroke study), the Figure 7a shows the change in tissue oxy-hemoglobin (*HbO*2) concentration at the lesioned and non-lesioned hemispheres from 0-60sec during the application of 0.526A/m^2 anodal tDCS from 0-30sec. Figure 7b shows the spectrogram illustrating non-stationary single-trial EEG at non-lesioned hemisphere where the 6th intrinsic mode function (IMF-6) primarily captured the temporal change in the power spectral density within 0.5Hz and 11.25 Hz (i.e., $IMF_{EEG,0.5-11.25Hz}$) during the application of 0.526A/m^2 anodal tDCS from 0-30sec. An immediate increase in the theta band (4Hz-8Hz) EEG activity after the start of anodal tDCS was found at the non-lesioned hemisphere. The Figure 7c shows the corresponding spectrograms for the lesioned hemisphere.

CCF analysis revealed a significant (95 percent confidence interval) negative cross-correlation at the non-lesioned hemisphere during anodal tDCS where the log-transformed mean-power of $IMF_{EEG,0.5-11.25Hz}$ lagged *HbO*2 (see Table 3). However, the CCF analysis did not reveal any significant cross-correlation beyond the upper and lower 95 percent confidence bounds at the lesioned hemisphere, assuming that $IMF_{EEG,0.5-11.25Hz}$ and *HbO*2 are completely uncorrelated. The CCF results during anodal tDCS at the non-lesioned hemisphere from all the trials (N = 15) for all the four cases are listed in Table 3. Here, the lag for Case-1 (0.93 ± 1.26sec) differed from the other cases which were comparable.

IV. DISCUSSION

In this paper, we presented development of a non-invasive point-of-care test (POCT) device to investigate neurovascular coupling (NVC) from simultaneous recording of EEG and NIRS responses evoked with tDCS that can avoid

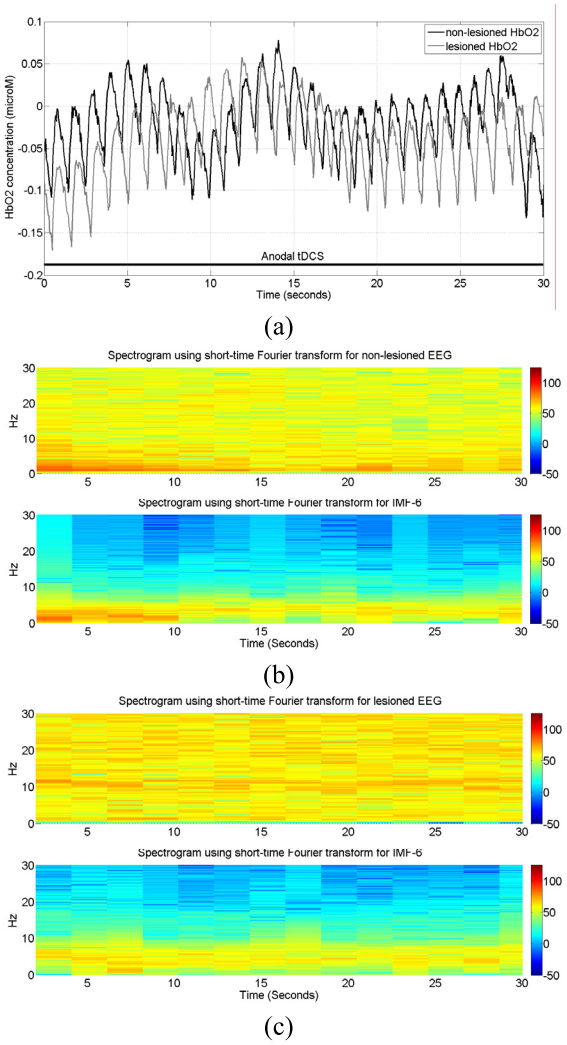

FIGURE 7. NIRS-EEG recording during anodal tDCS. a) Change in tissue oxy-hemoglobin (HbO_2) concentration at lesioned/affected and non-lesioned/healthy hemisphere. b) Spectrogram showing non-stationary single-trial EEG at non-lesioned hemisphere. The 6th intrinsic mode function (IMF-6) primarily captured the temporal change in the power spectral density. c) Spectrogram showing non-stationary single-trial EEG at lesioned hemisphere alongwith IMF-6.

transportation of critically ill patients. NIRS recorded changes in oxy-haemoglobin and deoxy-haemoglobin concentrations during anodal tDCS-induced activation of the cortical region located under the stimulation electrode and in-between the light sources and detector [28] where the feasibility was shown by the NIRS-tDCS healthy study. EEG estimated the anodal tDCS-induced alterations of the underlying neuronal current generators in the cortical region located under the stimulation electrode and in-between the light sources and detectors where the feasibility was shown by the EEG-tDCS healthy study. The stroke studies (NIRS-tDCS stroke study and NIRS/EEG-tDCS stroke study) showed detectable neural and hemodynamic changes to 0.526A/m^2 anodal tDCS in stroke survivors where the lesioned

TABLE 2. SNR of the 15 healthy subjects during on and off phases of TDCS.

Subject Id	Off-tDCS SNR (dB)	On-tDCS SNR (dB)
1	38.0721	39.9504
2	39.4715	41.5991
3	39.8311	41.3332
4	42.384	43.2835
5	41.2198	42.3838
6	39.5062	40.6702
7	40.819	42.5564
8	42.2779	45.4101
9	41.1092	42.3265
10	42.1952	44.1645
11	40.2977	42.4342
12	42.0211	42.963
13	40.1072	42.1107
14	40.1425	41.5978
15	40.5357	42.1622

TABLE 3. Summary of the results from the case series.

Case	Correlation Coefficient	Lag (sec)
1	-0.66±0.18	1.19±1.45
2	-0.63±0.14	3.48±1.57
3	-0.56±0.17	3.75±1.83
4	-0.58±0.12	3.83±1.76

hemisphere had a reduced tDCS-evoked hemodynamic response than the non-lesioned hemisphere (NIRS-tDCS stroke study). In the bi-hemispheric tDCS and simultaneous EEG-NIRS recording montage (NIRS/EEG-tDCS stroke study), we limited the number of NIRS detectors to 2, NIRS sources to 8, and EEG channels to 8 to reduce the cost as well as the complexity. For NIRS-EEG joint imaging, EEG captured the neuronal response and NIRS captured the hemodynamic response that were evoked with anodal tDCS which was shown to be technically feasible in laboratory setting without any artifacts from one other.

For calibrating the NIRS device, we developed a novel NIRS phantom that emulated the dynamic variation of cerebral oxygen saturation. However, one of the limitations of the phantom was that it only accounted for the isotropic response of the brain. The phantom did not take into account the cerebro-spinal fluid, which may also alter the scattering and absorption coefficients. Nevertheless, the results of phantom simulation studies indicated physiological 58% and 62% mean cerebral oxygen saturation when the optical properties of the phantom changed on being heated by resistive mesh through current stimulation. Following calibration with the NIRS phantom, the NIRS device was used for capturing cerebrovascular reactivity (CVR) [35]. It was

IEEE Journal of Translational Engineering in Health and Medicine

postulated that hemodynamic alterations are causally related to tDCS-induced neural alterations in cortical excitability via neuro-vascular coupling (NVC). In fact, the regional CVR during anodal tDCS was estimated with a phenomological model [35] that was developed by adapting an arteriolar compliance model of the cerebral blood flow response to neural stimulus [47]. The regional CVR was defined as the coupling between changes in cerebral blood flow (CBF) and cerebral metabolic rate of oxygen (CMRO2) during anodal tDCS-induced local brain activation [48]. In the current study, the mean SNR of the NIRS device was found to be 42.33 ± 1.33dB in the on state of tDCS and 40.67 ± 1.23dB in the off state of tDCS (see Table 2) where the difference was found to be statistically significant ($p < 0.01$). Also, the cerebral oxygenation level of the 15 healthy subjects was found in the range of 60-69%. The clinical study conducted on 14 stroke patients revealed that the lesioned hemisphere with impaired circulation showed significantly ($p < 0.01$) less change in cerebral oxygenation than the non-lesioned side in response to anodal tDCS.

Moreover, EEG can improve the sensitivity where topographic EEG has been found useful in brain ischemia [49]. The EEG power spectrum in healthy showed a statistically significant ($p < 0.05$) decrease around ''individual alpha frequency'' in the Alpha band (8-13Hz) following anodal tDCS. It was postulated based on prior work [50], [51] that anodal tDCS enhanced activity, and excitability of neurons at a population level in a non-specific manner, where μ-rhythm desynchronization was suggested to be generated [36]. For joint analysis of EEG-NIRS responses to tDCS, a method was developed leveraging Empirical Mode Decomposition (EMD) of the EEG time series to assess NVC using cross-correlation function (CCF) between mean (cortical) tissue oxy-(*HbO*2) haemoglobin concentration time-series and averaged PSD time-course from relevant intrinsic mode function (e.g. within 0.5Hz and 11.25 Hz). Here, CCF analysis revealed a significant negative cross-correlation only at the non-lesioned hemisphere at 95 percent confidence interval. Moreover, the CCF based assessment of the patient-specific cerebral microvessel status was found to be sensitive to white matter hyperintensities with suspected Cerebral Autosomal-Dominant Arteriopathy with Subcortical Infarcts and Leukoencephalopathy (CADASIL) in Case 1 where confirmatory studies are required. CADASIL condition affects blood flow in small blood vessels, particularly cerebral vessels within the brain [52]. In CADASIL, both basal perfusion and hemodynamic reserve are decreased [52] and this hypoperfusion may be related to the clinical severity.

However, the mechanism of tDCS action on NIRS remains unclear where a recent study [53] demonstrated consensual changes in heart rate variability during unilateral anodal tDCS. Here, an index of CVR based on low-frequency correlation of arterial blood pressure and *Hbt* measured with NIRS [54] can be used. Therefore, analog arterial pressure data from the operating room hemodynamic monitor was acquired along with NIRS in this current study which is currently being analysed to elucidate the mechanisms. Furthermore, the frequently observed initial dip in *HbO*2 at the beginning of anodal tDCS [43] may primarily be related to a fast local increase in total hemoglobin concentration due to vasodilation where the magnitude of the initial dip may reflect the temporal interplay of monophasic oxy-, deoxy-, and total haemoglobin signals, as elucidated by Sirotin et al. [55]. We postulated in our prior works [28], [43] that this initial dip which corresponded with an increase in the log-transformed mean-power of EEG within 0.5Hz-11.25Hz frequency band may be a biomarker of cerebral microvessel functionality (and NVC). Here, we proposed a phenomological model [35] based on the Friston's model [56] that anodal tDCS effected changes in synaptic transmembrane current led to a change in CBF via a change in the representative radius of the vasculature, and not in arterial and venous blood pressure difference. Also, it was assumed that the changes from baseline in *HbO*2 during anodal tDCS were solely due to local hemodynamic effect induced by anodal tDCS and not due to changes in arterial oxygen concentration. However, to understand the underlying mechanisms in it entirety, NIRS-EEG joint imaging presented in this paper may help in developing a simplified model for the complex path of NVC from a change in synaptic transmembrane current to a change in the concentration of multiple vasoactive agents (such as NO, potassium ions, adenosine) represented by a single vascular flow-inducing vasoactive signal that can be captured by the phenomological model [35] based on the first-order Friston's model [56].

In this study, we assumed that the spatially resolved spectroscopy technique removed skin blood flow artifacts from the NIRS signal but it needs to be verified with time-gated optical system for depth-resolved NIRS [39]. If needed, short separation NIRS channels can be added to regress out superficial extra-cortical contributions [40]. However, EEG-NIRS based NVC estimation revealed an interplay between impaired circulation and impaired neuronal response to anodal tDCS in the current study which is postulated to be robust to superficial extra-cortical contributions (e.g. CCF analysis may filter out electromyogram and skin blood flow artifacts). These need to be investigated further towards development of a robust biomarker for impaired cerebral microvessels and impaired neuronal functionality preceding cerebrovascular accident. Such impairments have been associated with increased risk of ischemic events and may help in stratifying stroke risk in patients with high-grade internal carotid artery stenosis or occlusion. Furthermore, it is postulated that the degree of NVC, estimated using simultaneous EEG and NIRS recordings, can be used to titrate anodal tDCS as a treatment to maximize blood perfusion in the lesioned region and surrounding ischemic penumbra by increasing local CBF [35]. This lends to a non-invasive bedside test and intervention device to localize the impaired circulation and impaired neuronal response in ischemic stroke and then target that with tDCS. Here, the frequency, symmetry and reactivity of neuronal and hemodynamics responses

evoked with tDCS may be the biomarker for our future field studies. In field studies, a tight hairnet over the sensor montage can help in preventing lift-off of the sensors and we are also developing robust sensor-fault tolerant algorithms for EEG-NIRS sensor fusion based on Kalman filters [59].

V. CONCLUSION

The paper presented a point of care testing device for neurovascular coupling (NVC) from simultaneous recording of electroencephalogram (EEG) and near infra red spectroscopy (NIRS) during anodal transcranial direct current stimulation (tDCS). The healthy and stroke study showed detectable neural and hemodynamic changes to $0.526 A/m^2$ anodal tDCS which demonstrated the feasibility of this technique. Moreover, it was shown in stroke survivors that the lesioned hemisphere with impaired circulation responded with significantly ($p < 0.01$) less change in cerebral oxygenation than the non-lesioned side to anodal tDCS where joint analysis of NIRS responses in conjunction with EEG was sensitive to white matter hyperintensities condition in a stroke survivors. Therefore, it can be concluded that anodal tDCS can perturb local neural and vascular activity (via NVC) which can be used for assessing regional cerebral microvessels functionality where confirmatory clinical studies are required in small vessel diseases.

ACKNOWLEDGMENT

Dr. A. Dutta would like to thank Prof. M. A. Nitsche for the discussions on the application of non-invasive brain stimulation techniques towards this work. The development of the EEG instrumentation (EEG-tDCS healthy study) and the NIRS-EEG system integration (NIRS/EEG stroke study) were performed under Dr. A. Dutta at the NeuroPhys4NeuroRehab team of INRIA, France where the technical help received from - R. Sehgal, G. Aggarwal, and A. Jacob - is gratefully acknowledged. The help received from the Neuro Rehab Services LLP, India and the Institute of Neurosciences Kolkata, India in conducting the preliminary NIRS/EEG stroke study is also gratefully acknowledged.

REFERENCES

[1] P. M. Dalal *et al.*, "Population-based stroke survey in Mumbai, India: Incidence and 28-day case fatality," *Neuroepidemiology*, vol. 31, no. 4, pp. 254–261, 2008.

[2] S. K. Das *et al.*, "A prospective community-based study of stroke in Kolkata, India," *Stroke*, vol. 38, no. 3, pp. 906–910, Mar. 2007.

[3] S. E. Sridharan *et al.*, "Incidence, types, risk factors, and outcome of stroke in a developing country: The Trivandrum Stroke Registry," *Stroke*, vol. 40, no. 4, pp. 1212–1218, Apr. 2009.

[4] A. D. Lopez, C. D. Mathers, M. Ezzati, D. T. Jamison, and C. J. Murray, "Global and regional burden of disease and risk factors, 2001: Systematic analysis of population health data," *Lancet*, vol. 367, no. 9524, pp. 1747–1757, May 2006.

[5] C. Benesch and R. G. Holloway, "Economic impact of stroke and implications for interventions," *CNS Drugs*, vol. 9, no. 1, pp. 29–39, Jun. 1998.

[6] A. S. Go *et al.*, "Heart disease and stroke statistics—2014 update: A report from the American Heart Association," *Circulation*, vol. 129, no. 3, pp. e28–e292, Jan. 2014.

[7] M. Tripathi and D. Vibha, "Stroke in young in India," *Stroke Res. Treat.*, vol. 2011, Dec. 2010.

[8] A. Das, A. L. Botticello, G. R. Wylie, and K. Radhakrishnan, "Neurologic disability: A hidden epidemic for India," *Neurology*, vol. 79, no. 21, pp. 2146–2147, Nov. 2012.

[9] *WG-3.2 Non-Communicable Diseases Report*. [Online]. Available: http://planningcommission.nic.in/aboutus/committee/wrkgrp12/health/WG_3_2non_communicable.pdf, accessed Aug. 23, 2014.

[10] H. Markus and M. Cullinane, "Severely impaired cerebrovascular reactivity predicts stroke and TIA risk in patients with carotid artery stenosis and occlusion," *Brain*, vol. 124, no. 3, pp. 457–467, Mar. 2001.

[11] K. A. Hossmann, "Viability thresholds and the penumbra of focal ischemia," *Ann. Neurol.*, vol. 36, no. 4, pp. 557–565, Oct. 1994.

[12] J. Astrup, B. K. Siesjö, and L. Symon, "Thresholds in cerebral ischemia—The ischemic penumbra," *Stroke*, vol. 12, no. 6, pp. 723–725, Nov. 1981.

[13] L. B. Goldstein, "Should antihypertensive therapies be given to patients with acute ischemic stroke?" *Drug Safety*, vol. 22, no. 1, pp. 13–18, Jan. 2000.

[14] S. L. Dawson, R. B. Panerai, and J. F. Potter, "Serial changes in static and dynamic cerebral autoregulation after acute ischaemic stroke," *Cerebrovascular Diseases*, vol. 16, no. 1, pp. 69–75, 2003.

[15] H. Girouard and C. Iadecola, "Neurovascular coupling in the normal brain and in hypertension, stroke, and Alzheimer disease," *J. Appl. Physiol.*, vol. 100, no. 1, pp. 328–335, Jan. 2006.

[16] M. Silvestrini *et al.*, "Cerebrovascular reactivity and cognitive decline in patients with Alzheimer disease," *Stroke*, vol. 37, no. 4, pp. 1010–1015, Apr. 2006.

[17] S. Lloyd-Fox, A. Blasi, and C. E. Elwell, "Illuminating the developing brain: The past, present and future of functional near infrared spectroscopy," *Neurosci. Biobehavioral Rev.*, vol. 34, no. 3, pp. 269–284, Mar. 2010.

[18] M. T. Douds, E. J. Straub, A. C. Kent, C. H. Bistrick, and J. J. Sistino, "A systematic review of cerebral oxygenation-monitoring devices in cardiac surgery," *Perfusion*, vol. 29, no. 6, pp. 545–552, 2014.

[19] A. Villringer and B. Chance, "Non-invasive optical spectroscopy and imaging of human brain function," *Trends Neurosci.*, vol. 20, no. 10, pp. 435–442, Oct. 1997.

[20] X. Zheng, D. C. Alsop, and G. Schlaug, "Effects of transcranial direct current stimulation (tDCS) on human regional cerebral blood flow," *Neuroimage*, vol. 58, no. 1, pp. 26–33, Sep. 2011.

[21] S. Coyle, T. Ward, C. Markham, and G. McDarby, "On the suitability of near-infrared (NIR) systems for next-generation brain-computer interfaces," *Physiol. Meas.*, vol. 25, no. 4, pp. 815–822, Aug. 2004.

[22] G. Buzsáki, C. A. Anastassiou, and C. Koch, "The origin of extracellular fields and currents—EEG, ECoG, LFP and spikes," *Nature Rev. Neurosci.*, vol. 13, no. 6, pp. 407–420, Jun. 2012.

[23] B. Foreman and J. Claassen, "Quantitative EEG for the detection of brain ischemia," *Crit Care*, vol. 16, no. 2, p. 216, Mar. 2012.

[24] R. V. Sheorajpanday, G. Nagels, A. J. Weeren, M. J. van Putten, and P. P. De Deyn, "Reproducibility and clinical relevance of quantitative EEG parameters in cerebral ischemia: A basic approach," *Clin. Neurophysiol., Off. J. Int. Fed. Clin. Neurophysiol.*, vol. 120, no. 5, pp. 845–855, May 2009.

[25] K. Jann, T. Koenig, T. Dierks, C. Boesch, and A. Federspiel, "Association of individual resting state EEG alpha frequency and cerebral blood flow," *Neuroimage*, vol. 51, no. 1, pp. 365–372, May 2010.

[26] J. A. Filosa, "Vascular tone and neurovascular coupling: Considerations toward an improved *in vitro* model," *Frontiers Neuroenergetics*, vol. 2, Aug. 2010.

[27] R. L. Barbour *et al.*, "A programmable laboratory testbed in support of evaluation of functional brain activation and connectivity," *IEEE Trans. Neural Syst. Rehabil. Eng.*, vol. 20, no. 2, pp. 170–183, Mar. 2012.

[28] A. Dutta, "EEG-NIRS based low-cost screening and monitoring of cerebral microvessels functionality," in *Proc. Int. Stroke Conf.*, 2014.

[29] B. Molaee-Ardekani *et al.*, "Effects of transcranial Direct Current Stimulation (tDCS) on cortical activity: A computational modeling study," *Brain Stimul.*, vol. 6, no. 1, pp. 25–39, Jan. 2013.

[30] C. G. Carvalhaes and P. Suppes, "A spline framework for estimating the EEG surface Laplacian using the Euclidean metric," *Neural Comput.*, vol. 23, no. 11, pp. 2974–3000, Nov. 2011.

[31] F. Perrin, J. Pernier, O. Bertrand, and J. F. Echallier, "Spherical splines for scalp potential and current density mapping," *Electroencephalogr. Clin. Neurophysiol.*, vol. 72, no. 2, pp. 184–187, Feb. 1989.

[32] A. Dutta and M. A. Nitsche, "Neural mass model analysis of online modulation of electroencephalogram with transcranial direct current stimulation," in *Proc. 43rd Annu. Meeting Soc. Neurosci.*, 2013.

IEEE Journal of Translational Engineering in Health and Medicine

[33] M. A. Nitsche and W. Paulus, "Excitability changes induced in the human motor cortex by weak transcranial direct current stimulation," *J. Physiol.*, vol. 527, pp. 633–639, Sep. 2000.

[34] D. Wachter *et al.*, "Transcranial direct current stimulation induces polarity-specific changes of cortical blood perfusion in the rat," *Experim. Neurol.*, vol. 227, no. 2, pp. 322–327, Feb. 2011.

[35] A. Dutta, S. R. Chowdhury, A. Dutta, P. N. Sylaja, D. Guiraud, and M. A. Nitsche, "A phenomological model for capturing cerebrovascular reactivity to anodal transcranial direct current stimulation," in *Proc. 6th Int. IEEE/EMBS Conf. Neural Eng. (NER)*, Nov. 2013, pp. 827–830.

[36] A. Dutta and M. A. Nitsche, "Neural mass model analysis of online modulation of electroencephalogram with transcranial direct current stimulation," in *Proc. 6th Int. IEEE/EMBS Conf. Neural Eng. (NER)*, Nov. 2013, pp. 206–210.

[37] C. D. Kurth, H. Liu, W. S. Thayer, and B. Chance, "A dynamic phantom brain model for near-infrared spectroscopy," *Phys. Med. Biol.*, vol. 40, no. 12, pp. 2079–2092, Dec. 1995.

[38] X. Xu *et al.*, "Validation of NIRS in measuring tissue hemoglobin concentration and oxygen saturation on ex vivo and isolated limb models," *Proc. SPIE*, vol. 4955, pp. 369–378, Jul. 2003.

[39] R. L. Barbour *et al.*, "Validation of near infrared spectroscopic (NIRS) imaging using programmable phantoms," *Proc. SPIE*, vol. 6870, pp. 687002-1–687002-10, Feb. 2008.

[40] P. H. Koh, C. E. Elwell, and D. T. Delpy, "Development of a dynamic test phantom for optical topography," in *Oxygen Transport to Tissue 30*, P. Liss, P. Hansell, D. F. Bruley, and D. K. Harrison, Eds. New York, NY, USA: Springer-Verlag, 2009, pp. 141–146.

[41] *Photon Migration Imaging Toolbox Homepage*. [Online]. Available: http://www.nmr.mgh.harvard.edu/PMI/toolbox/, accessed Aug. 23, 2014.

[42] A. Viswanathan and R. D. Freeman, "Neurometabolic coupling in cerebral cortex reflects synaptic more than spiking activity," *Nature Neurosci.*, vol. 10, no. 10, pp. 1308–1312, Oct. 2007.

[43] A. Dutta, A. Jacob, S. R. Chowdhury, A. Das, and M. A. Nitsche, "EEG-NIRS based assessment of neurovascular coupling during anodal transcranial direct current stimulation—A stroke case series," *J. Med. Syst.*, 2014.

[44] A. Delorme and S. Makeig, "EEGLAB: An open source toolbox for analysis of single-trial EEG dynamics including independent component analysis," *J. Neurosci. Methods*, vol. 134, no. 1, pp. 9–21, Mar. 2004.

[45] N. E. Huang *et al.*, "The empirical mode decomposition and the Hilbert spectrum for nonlinear and non-stationary time series analysis," *Proc. Roy. Soc. London Ser. A, Math., Phys. Eng. Sci.*, vol. 454, no. 1971, pp. 903–995, Mar. 1998.

[46] H. An and W. Lin, "Quantitative measurements of cerebral blood oxygen saturation using magnetic resonance imaging," *J. Cerebral Blood Flow Metabolism, Off. J. Int. Soc. Cerebral Blood Flow Metabolism*, vol. 20, no. 8, pp. 1225–1236, Aug. 2000.

[47] Y. Behzadi and T. T. Liu, "An arteriolar compliance model of the cerebral blood flow response to neural stimulus," *Neuroimage*, vol. 25, no. 4, pp. 1100–1111, May 2005.

[48] O. Leontiev and R. B. Buxton, "Reproducibility of BOLD, perfusion, and CMRO2 measurements with calibrated-BOLD fMRI," *Neuroimage*, vol. 35, no. 1, pp. 175–184, Mar. 2007.

[49] K. Nagata, "Topographic EEG in brain ischemia—Correlation with blood flow and metabolism," *Brain Topogr.*, vol. 1, no. 2, pp. 97–106, 1988.

[50] F. H. Lopes da Silva, A. van Rotterdam, P. Barts, E. van Heusden, and W. Burr, "Models of neuronal populations: The basic mechanisms of rhythmicity," *Progr. Brain Res.*, vol. 45, pp. 281–308, 1976.

[51] J. Matsumoto, T. Fujiwara, O. Takahashi, M. Liu, A. Kimura, and J. Ushiba, "Modulation of mu rhythm desynchronization during motor imagery by transcranial direct current stimulation," *J. Neuroeng. Rehabil.*, vol. 7, p. 27, Jun. 2010.

[52] H. Chabriat *et al.*, "Cerebral hemodynamics in CADASIL before and after acetazolamide challenge assessed with MRI bolus tracking," *Stroke*, vol. 31, no. 8, pp. 1904–1912, Aug. 2000.

[53] R. A. Montenegro *et al.*, "Transcranial direct current stimulation influences the cardiac autonomic nervous control," *Neurosci. Lett.*, vol. 497, no. 1, pp. 32–36, Jun. 2011.

[54] J. K. Lee *et al.*, "Cerebrovascular reactivity measured by near-infrared spectroscopy," *Stroke*, vol. 40, no. 5, pp. 1820–1826, May 2009.

[55] Y. B. Sirotin, E. M. C. Hillman, C. Bordier, and A. Das, "Spatiotemporal precision and hemodynamic mechanism of optical point spreads in alert primates," *Proc. Nat. Acad. Sci. United States Amer.*, vol. 106, no. 43, pp. 18390–18395, Oct. 2009.

[56] K. J. Friston, A. Mechelli, R. Turner, and C. J. Price, "Nonlinear responses in fMRI: The Balloon model, Volterra kernels, and other hemodynamics," *Neuroimage*, vol. 12, no. 4, pp. 466–477, Oct. 2000.

[57] J. Selb, D. K. Joseph, and D. A. Boas, "Time-gated optical system for depth-resolved functional brain imaging," *J. Biomed. Opt.*, vol. 11, no. 4, p. 044008, Aug. 2006.

[58] L. Gagnon, R. J. Cooper, M. A. Yücel, K. L. Perdue, D. N. Greve, and D. A. Boas, "Short separation channel location impacts the performance of short channel regression in NIRS," *Neuroimage*, vol. 59, no. 3, pp. 2518–2528, Feb. 2012.

[59] A. Dutta, K. Koerding, E. Perreault, and L. Hargrove, "Sensor-fault tolerant control of a powered lower limb prosthesis by mixing mode-specific adaptive Kalman filters," in *Proc. Annu. Int. Conf. IEEE Eng. Med. Biol. Soc.*, vol. 2011. Aug./Sep. 2011, pp. 3696–3699.

UTKARSH JINDAL was born in 1993. He is currently pursuing the M.S. degree in electronics and communication engineering from the International Institute of Information Technology, Hyderabad, India. His research interests span around the development of embedded systems for biomedical applications. His aim is to provide low-cost devices for medical diagnosis for the common people.

MEHAK SOOD was born in 1991. She is currently pursuing the M.S. degree in electronics and communication engineering from the International Institute of Information Technology, Hyderabad, India. Her field of interest is mainly in developing solutions to the healthcare needs from her knowledge in embedded system design. She intends to reach the poor section of society too who do not afford expensive healthcare services.

ANIRBAN DUTTA received the Ph.D. degree from the Department of Biomedical Engineering, Case Western Reserve University, Cleveland, OH, USA, in 2008. He is currently the Principal Investigator of the Institut National de Recherche en Informatique et en Automatique's NeuroPhys4NeuroRehab project with the DEMAR Research Group, Montpellier Laboratory of Informatics, Robotics, and Microelectronics, Montpellier, France, a cross-faculty research entity of the University of Montpellier 2, Montpellier, and the National Center for Scientific Research—Institut des Sciences Informatiques et de Leurs Interactions, Paris, France. His research interests are in biosignals processing and human–motor control, electrical neuromodulation devices, gait biomechanics and dynamics, clinical neurophysiology, and computational neurosciences.

SHUBHAJIT ROY CHOWDHURY (M'13) was born in 1981. He received the Ph.D. degree from the Department of Electronics and Telecommunication Engineering, Jadavpur University, Kolkata, India, in 2010.

He is currently an Assistant Professor with the Centre for VLSI and Embedded Systems Technology, International Institute of Information Technology, Hyderabad, India. He was a Lecturer with Jadavpur University from 2006 to 2010. His research interests span around the development of biomedical embedded systems, very large scale integration (VLSI) architectures, and application specified integrated circuit design of intelligent signal processing circuits. He is keenly interested in the educational system and its necessary transformation. He has authored over 75 papers in international journals and conferences.

Dr. Roy Chowdhury is a member of the VLSI Society of India, and a Life Member of the Indian Statistical Institute, the Microelectronics Society of India, and the Telemedicine Society of India. He is a member of the Scientific, Technical, and Editorial Committee of the Engineering and Natural Sciences Division of the World Academy of Engineering, Science and Technology. He was a recipient of the University Gold Medals for his B.E. and M.E. degrees, in 2004 and 2006, respectively, the Altera Embedded Processor Designer Award in 2007, and a winner of four best paper awards. He received the award of the Fellow of Society of Applied Biotechnology by the Society of Applied Biotechnology in 2012. He was also a recipient of the Young Engineers' Award by the Institution of Engineers of India for his outstanding contribution in Electronics and Telecommunication Engineering from 2012 to 2013. He is a reviewer of the IEEE TRANSACTIONS ON VERY LARGE SCALE INTEGRATION SYSTEMS, the *ACM Transactions on Design Automation of Electronic Systems*, *Medical Systems, Medical and Biological Engineering and Computing* journal, *Computers in Biology and Medicine*, *Computers Methods and Programs in Biomedicine*, and other reputed journals.